A geometric approach to the static balancing of mechanisms constructed using spherical kinematic chain units

A geometric approach to the static balancing of mechanisms constructed using spherical kinematic chain units

Jieyu Wang[1,2], Xianwen Kong[2*]

1. Robotics Institute, School of Mechanical Engineering and Automation, Beihang University, Beijing 100191, China
2. School of Engineering and Physical Sciences, Heriot-Watt University, Edinburgh EH14 4AS UK

Abstract

A geometric method to the static balancing of spherical mechanisms constructed using spherical chain units is presented. A spherical kinematic chain unit is composed of n moving links, whose masses are considered, connected by revolute (R) joints of which the axes intersect at a fixed point. The mass of each link can be balanced using one spring without any auxiliary parallelograms. The balancing can be achieved readily with almost no calculation. One end of each spring is fixed right above the intersection of the joint axes and the other end is attached to the point that is on the line defined by the intersection and the equivalent center of mass of the corresponding link (combining the masses of the link and the payload). This method is then applied to the mechanisms constructed using spherical kinematic chain units, and the ones constructed using spherical kinematic chain units and other types of kinematic chain units. By distributing the mass of a link onto its adjacent links, balancing of the mechanism is reduced to those of several spherical kinematic chain units, which can be balanced using the proposed method. Two examples are given, including a Bennett plano-spherical hybrid linkage and a 3-RRS parallel mechanism to illustrate the proposed method for static balancing.

Keywords

Static balancing, springs, spherical mechanisms, mass moment substitution

1. Introduction

Mechanisms are said to be statically balanced when the potential energy is constant. This condition is also referred to as gravity compensation. Static balancing leads to low actuation forces required to move the devices, and therefore improve efficiency. The 1-degree-of-freedom (DOF) one-link mechanism has already been perfectly balanced, using zero-free-length springs (free-length of the spring is equal to zero) [1], counterweights [2], cams [3] and gears [4].

The total weight and inertia of the device are lower when using springs, compared with using counterweights. One of the best-known statically balanced devices using springs is the Anglepoise lamp designed by Carwardine [5, 6]. The balanced devices with springs were also applied to laparoscope holders used for minimally invasive surgery [7], exoskeleton [8], and limb/arm assist devices [9-11].

Gosselin and Wang [12-14] introduced a family of gravity-balanced parallel mechanisms (PMs), including 3-DOF, 4-DOF and 6-DOF spatial PMs, of which the balancing conditions were derived by solving the potential energy equations. In [15], 3-DOF 1-link spherical manipulators and spherical PMs, in which only the masses of the moving platforms were considered, were balanced. Herder et al [16-17] mainly focused on the planar manipulators, as well as the spatial ones composed of planar chains. Lin et al [18, 19] demonstrated several statically balanced spatial manipulators, whose design parameters were obtained by diagonalizing the stiffness matrix. Agrawal and Fattah [20] investigated the gravity-balancing of the 2-DOF and 3-DOF spatial manipulators, by identifying the center of mass (CM) through auxiliary parallelograms. Chung et al [21] described a gravity compensation mechanism for the robot arm with roll-pitch coupling rotation by using a Scotch Yoke mechanism. Walsh et al [22] put forward a general methodology

---

to design *n*-spring balancers for the 2-DOF manipulator with yaw-pitch rotation. Cho et al [23] designed a gravity compensator for the arm with roll-pitch rotation. The system is comprised of two 1-DOF gravity compensators and a bevel differential. Based on the work of [23], a 4-DOF manipulator was developed in [24]. For the manipulators with variable payloads, different balancing approaches were also discussed in [25-32].

The balancing methods for spatial manipulators in the literature require either derivation using the algebraic method or auxiliary links. Lin et al [33] derived the balancing conditions for an *n*-link manipulator using *n* springs. However, the balancing of each link in [33] should not be regarded as independent, and the systems are not statically balanced unless considering only the mass of the payload and neglecting the mass of each link.

This paper proposes a general method to design statically balanced *n*-DOF spherical multi-link manipulators readily and quickly, using a geometric method. Only springs are used to balance all the links, whose masses are considered. No auxiliary parallelogram is required. The method is then extended to mechanisms composed of spherical kinematic chain units, and those composed of spherical kinematic chain units and other types of kinematic chain units. A spherical kinematic chain unit is composed of *n* moving links, whose masses are considered, connected by revolute (R) joints of which the axes intersect at a fixed point.

This paper is organized as follows: the method in [15] is extended to the static balancing of 2-DOF/3-DOF 2-link spherical manipulators in Section 2. In Section 3, the general method of static balancing of spherical manipulators is provided. The mechanisms constructed of spherical chain units are balanced in Section 4. The mass moment substitution approaches and the statically balanced mechanisms constructed using spherical chain units and other types of chain units are presented in Section 5. Finally, conclusions are drawn.

2. Extension of the Gosselin method for static balancing of a rotating link

2.1 The Gosselin method for static balancing of a rotating link

According to [15], a link manipulator mounted to the base using a spherical (S) joint can be statically balanced using only one zero-free-length spring. A zero-free-length spring can be realized using guiding systems or pulleys and wires [34]. The spring connecting point *H* on the base is right above the S joint and the height is assumed to be *h*. *b* is the position vector of the spring connecting point on the manipulator and *r* is the position vector of the CM of the manipulator. Vectors *b* and *r* must be proportional [15], i.e.,

$$r = (kh/mg)b \qquad (1)$$

where *m*, *g* and *k* represent the mass of the manipulator, the gravitational acceleration, and the stiffness of spring respectively. The spring connecting point on the manipulator should be on the line defined by the CM of the manipulator and the center of the S joint [Fig. 1(a)]. $h = mg/k$ when attaching the spring to the CM of the manipulator directly, for the sake of convenience of calculation and description [Fig. 1(b)]. This condition can also apply to one-link manipulators with a revolute (R) [16] and universal (U) joint.
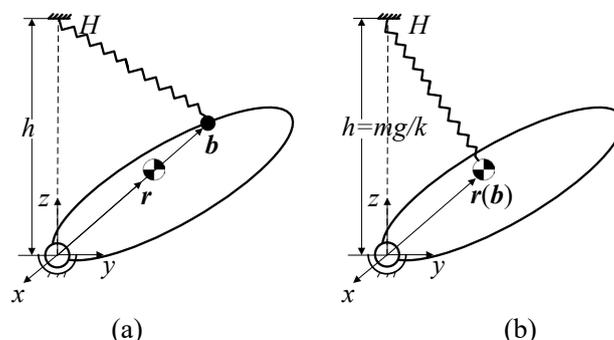

Fig. 1 Statically balanced 3-DOF 1-link manipulator: (a) the condition in [15]; (b) attaching the spring to the CM of the link

2.2 The extension of the Gosselin method

In this section, the condition in which there is no need to balance the links of the manipulator will be derived and the statically balanced 2-link and 3-link manipulators with intersecting joint axes will be constructed by using the balancing condition for a single link rotating about a fixed point [15]. For the 1-link mechanism mounted on the base using an R joint, the spring can be attached to an arbitrary point right above the axis of the R joint. As shown in Fig. 2(a), the angle between the axis of the R joint and the vertical axis is denoted by α (with constant value), and the position of the equivalent CM (combining the masses of the link and the payload) of the manipulator in the local coordinate frame is $\{a\ b\ c\}^T$. T is a point on the axis of the R joint, and $OT = t$ (a, b, c and t are with arbitrary values). H is right above T, with a distance of h. Now the special cases that no spring is required to balance the manipulator will be discussed.

A coordinate system is fixed to the base with its z-axis pointing vertically upward and with its origin located at O. Suppose the position vector of the equivalent CM of the ith link in the local frame i is represented by

$$^iP_i = \{a\quad b\quad c\}^T \tag{2}$$

The position vectors of the CMs of the links in the fixed frame can be obtained using the approach proposed by Denavit and Hartenberg [35]. The transfer matrix $^{i-1}_iT$ from the i-1th local frame to i^{th} local frame is described as

$$^{i-1}_iT = \begin{bmatrix} C\theta_i & -S\theta_i & 0 & l_{i-1} \\ C\alpha_{i-1}S\theta_i & C\alpha_{i-1}C\theta_i & -S\alpha_{i-1} & -d_iS\alpha_{i-1} \\ S\alpha_{i-1}S\theta_i & S\alpha_{i-1}C\theta_i & C\alpha_{i-1} & d_iC\alpha_{i-1} \\ 0 & 0 & 0 & 1 \end{bmatrix} \tag{3}$$

The position vectors of T, H and the equivalent CM of the manipulator P are computed as

$$T = \{0\quad -tS\alpha\quad tC\alpha\}^T \tag{4}$$

$$H = \{0\quad -tS\alpha\quad tC\alpha + h\}^T \tag{5}$$

$$\begin{Bmatrix} P \\ 1 \end{Bmatrix} = {}^0_1T\begin{Bmatrix} {}^1P_1 \\ 1 \end{Bmatrix} = \{aC\theta - bS\theta \quad bC\theta C\alpha - cS\alpha + aC\alpha S\theta \quad cC\alpha + bC\theta S\alpha + aS\theta S\alpha \quad 1\}^T \tag{6}$$

where C and S stand, respectively, for the cosine and the sine of the angles.
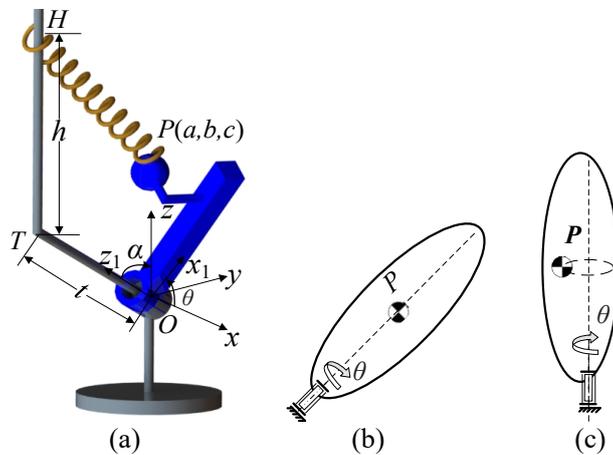

Fig. 2 Statically balanced 1-DOF 1-link manipulator: (a) the 3D model of the manipulator; (b) the CM of the link is on the joint axis; (c) the axis of the R joint is vertical

One spring is adopted, with one end attached to H, and the other end to the equivalent CM of the manipulator. The potential energy of the link consists of two parts, including the potential energy associated with gravity (V_{mi}) and the elastic potential energy stored in the springs (V_{si}). The total potential energy of the manipulator is yielded as

$$V = \frac{1}{2}k|P - H|^2 + mgP_z = \frac{1}{2}k[a^2 + b^2 + h^2 + (c - t)^2] + (-chk + mgc + hkt)C\alpha \\ -(hk - mg)S\alpha(bC\theta + aS\theta) \tag{7}$$

When the manipulator is statically balanced, the total potential energy should be constant. One can obtain that

$$h = mg/k \quad or \tag{8}$$

$$a = 0 \text{ and } b = 0 \quad or \tag{9}$$

$$\alpha = 0° \tag{10}$$

Equations (9) and (10) indicate that the system is balanced without spring if the CM of the link is on the joint axis [Fig. 2(b)], or the axis of the first R joint is vertical [Fig. 2(c)].

Based on the above results, the manipulators with yaw-roll rotation and yaw-pitch-roll rotation, constructed using the 1-DOF 1-link manipulator, can be easily balanced. The manipulator with yaw-roll rotation is comprised of two links and two orthogonal R joints, whose axes are vertical and horizontal respectively [Fig. 3(a)]. The manipulator with yaw-pitch-roll rotation, which is composed of one R joint and one U joint, is shown in Fig. 3(b). No spring is needed to balance the first link. The second link of each manipulator is balanced using one spring. The detailed analysis is given in Appendix A.
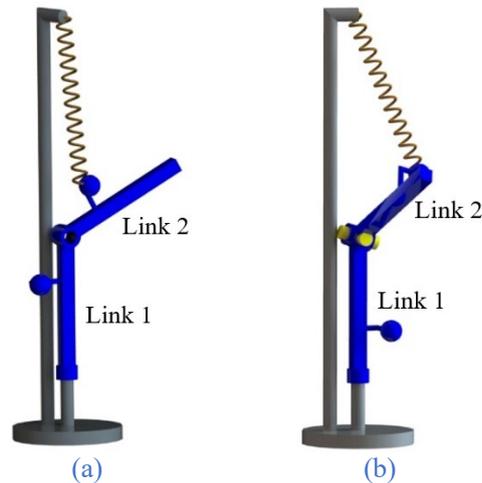

Fig. 3 Statically balanced 2-link manipulator: (a) yaw-roll rotation; (b) yaw-pitch-roll rotation

Now the balancing method for the 2-link manipulators in which the axis of the first R joint is horizontal will be investigated. The manipulator with pitch-roll rotation is shown in Fig. 4(a). It consists of two moving links connected by two R joints with intersecting and orthogonal axes. Two springs are used to balance the two links of the manipulator respectively. The spring connecting point on the base H_1 for the balancing of the first link can be any point right above the axis of the first R joint. The other end is attached to the CM of the first link. One end of the second spring H_2 is located on the vertical axis passing through the intersection of the two R joints, the other end is fixed on the CM of the second link.

The manipulator with pitch-yaw-roll rotation is shown in Fig. 4(b). The manipulator is a special case of the arm in [36]. Similarly, two springs are used to balance the two links of the manipulator respectively. One end of each spring is attached right above the joint, while the other end is fixed on the CM of the link. The detailed analysis is presented in Appendix A.
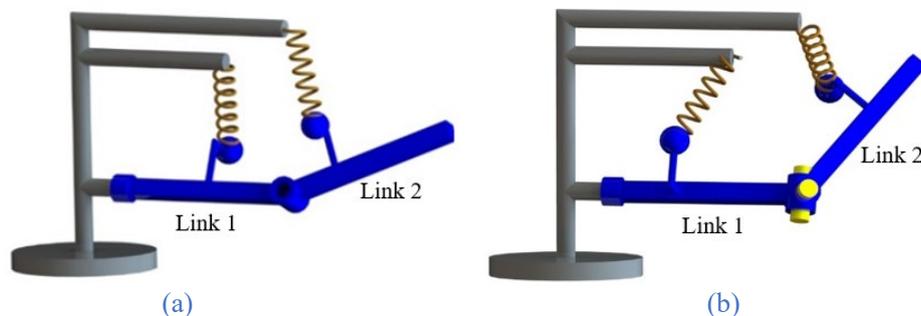
Fig. 4 Statically balanced 2-link manipulator: (a) pitch-roll rotation; (b) pitch-yaw-roll rotation

It is noteworthy that in theory, the spring connecting point on the link can be any point on the line defined by a point on the axis of the joint and the CM of the link when designing the system, and that on the base can be any points right above the joint axis with a certain height, as shown in Fig. 5(a). This condition is verified in Appendix B. For the sake of convenience of calculation and

description, the springs are attached to the equivalent CMs of the links in this paper. If an additional payload is added, as shown in Fig. 5(b), the method still works by identifying the combined CM of the second link.

<p align="center">(a)   (b)</p>

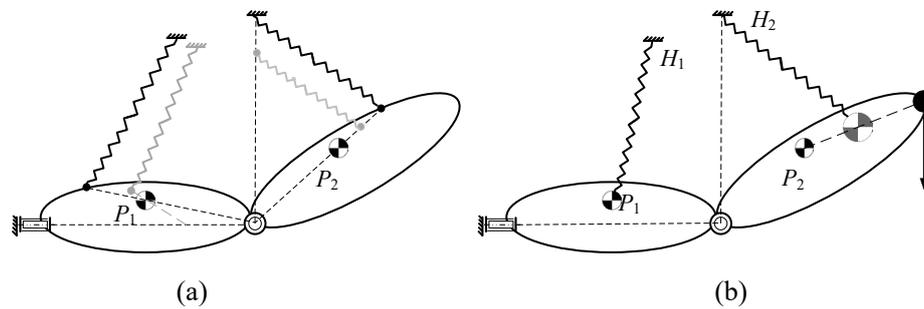Fig. 5 Extensions of the statically balanced 2-link manipulator with pitch-roll rotation: (a) attaching the spring to the point on the line defined by the centre of the joint and the CM of the link (two solutions); (b) with additional payload

3. Static balancing method of spherical manipulators

3.1 The static balancing approach of a general spherical manipulator

In Section 2, we have shown that the 2-link manipulators with intersecting joint axes can be balanced using one or two springs. The 2-link manipulators are special cases of spherical manipulators. In this section, the conditions of static balancing for a general spherical manipulator will be derived. In a general spherical manipulator, all the axes of R joints intersect at a point [Fig. 6(a)]. It has a remote center-of-motion (RCM). All the links move around the point of intersection, which is equivalent to a virtual S joint (the statically balanced mechanisms with S joints have been studied in [15]). It is hypothesized that all the spherical manipulators composed of n moving links can be balanced using n [or $(n-1)$] springs.

The general balancing method is: using one spring to balance each moving link of the manipulators. One end of the spring is attached to a point right above the intersection of the joint axes, the other end is fixed on the line defined by the intersection and the CM of the link. It is noted that the connecting point on the base for the first link can be any point on the line right above the axis of the first R joint, as shown in Fig. 6(a). If the manipulator has the same parameters as the 2-DOF/3-DOF spherical manipulators in Section 2, n-1 springs will be required for the static balancing.

<p align="center">(a)   (b)</p>

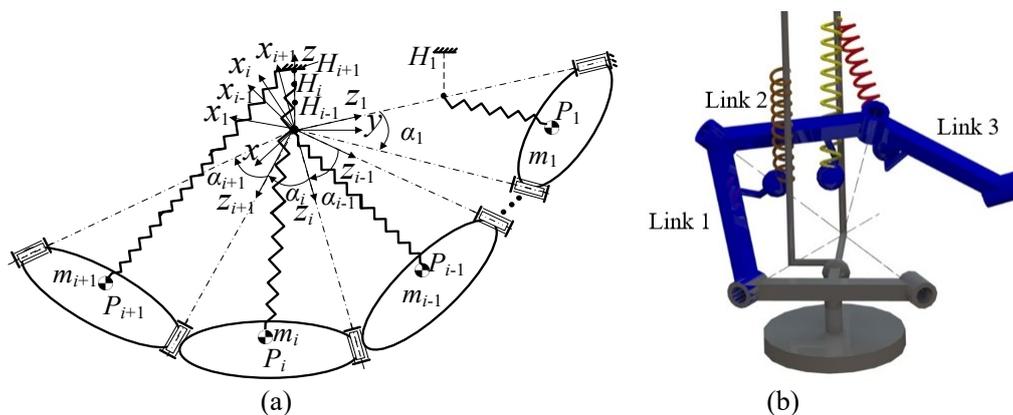Fig. 6 Statically balanced spherical manipulator: (a) the sketch of the manipulator; (b) the 3D model of the manipulator (case with three links)

To verify the system using the proposed method is valid, the total potential energy of the system will be proved to be constant. The link masses and joint twist angles of the manipulator are respectively noted as m_i and α_i, with arbitrary values ($i = 1, 2, 3\ldots$).

A global coordinate system is fixed to the base with its z-axis pointing vertically upward and with its origin located at the intersection of the axes of the R joints. Suppose the position vector of the CM (or equivalent CM) of the ith link in the local frame i is represented by

$$^i\boldsymbol{P_i} = \{a_i \quad b_i \quad c_i\}^T \tag{11}$$

The springs connecting points $\boldsymbol{H_i}$ on the base are all set to be

$$\boldsymbol{H_i} = \{0 \quad 0 \quad m_i g/k\}^T \quad (i = 1,2,3) \tag{12}$$

Take the first three links as examples to verify the balancing approach. Manipulator with three moving links and three R joints is illustrated in Fig. 6(b). The position vectors of the CMs of the three links in the global coordinate system are yielded as

$$\left\{ \begin{matrix} \boldsymbol{P_1} \\ 1 \end{matrix} \right\} = {}^0_1T \left\{ \begin{matrix} ^1\boldsymbol{P_1} \\ 1 \end{matrix} \right\} = \{-b_1 S\theta_1 + a_1 C\theta_1 \quad c_1 \quad -a_1 S\theta_1 - b_1 C\theta_1 \quad 1\}^T \tag{13}$$

$$\left\{ \begin{matrix} \boldsymbol{P_2} \\ 1 \end{matrix} \right\} = {}^0_1T\,{}^1_2T \left\{ \begin{matrix} ^2\boldsymbol{P_2} \\ 1 \end{matrix} \right\} = \{P_{2x} \quad (c_2 C\alpha_1 - b_2 S\alpha_1 C\theta_2 - a_2 S\alpha_1 S\theta_2)/2 \quad P_{2z} \quad 1\}^T \tag{14}$$

where

$$P_{2x} = [-S\theta_1(c_2 S\alpha_1 + b_2 C\alpha_1 C\theta_2 + a_2 C\alpha_1 S\theta_2) + C\theta_1(a_2 C\theta_2 - b_2 S\theta_2)]/2$$
$$P_{2z} = [C\theta_1(-c_2 S\alpha_1 + b_2 C\alpha_1 C\theta_2 + a_2 C\alpha_1 S\theta_2) + S\theta_1(-a_2 C\theta_2 + b_2 S\theta_2)]/2$$

$$\left\{ \begin{matrix} \boldsymbol{P_3} \\ 1 \end{matrix} \right\} = {}^0_1T\,{}^1_2T\,{}^2_3T \left\{ \begin{matrix} ^3\boldsymbol{P_3} \\ 1 \end{matrix} \right\} = \{P_{3x} \quad P_{3y} \quad P_{3z} \quad 1\}^T \tag{15}$$

where P_{3x}, P_{3y} and P_{3z} are given in Appendix B.

The potential energy of each link can be obtained as

$$V1 = \frac{1}{2}k|\boldsymbol{P_1} - \boldsymbol{H_1}|^2 + m_1 g P_{1z} = (a_1^2 k^2 + b_1^2 k^2 + c_1^2 k^2 + m_1^2 g^2)/2k \tag{16}$$

$$V2 = \frac{1}{2}k|\boldsymbol{P_2} - \boldsymbol{H_2}|^2 + m_2 g P_{2z} = (a_2^2 k^2 + b_2^2 k^2 + c_2^2 k^2 + m_2^2 g^2)/2k \tag{17}$$

$$V3 = \frac{1}{2}k|\boldsymbol{P_3} - \boldsymbol{H_3}|^2 + m_3 g P_{3z} = (a_3^2 k^2 + b_3^2 k^2 + c_3^2 k^2 + m_3^2 g^2)/2k \tag{18}$$

Similarly, we can verify that the potential energy of each link is a constant, and is equal to $(a_i^2 k^2 + b_i^2 k^2 + c_i^2 k^2 + m_i^2 g^2)/2k$. Therefore, the total potential energy of the spherical manipulator is a constant and the system designed is statically balanced.

Taking a serial spherical manipulator as a spherical kinematic chain unit, the above result on the static balancing of serial spherical manipulator can be used in the static balancing of single-loop mechanisms that can be decomposed into one or two spherical kinematic chain units by disconnecting one joint in Sections 3.2 and 3.3 and static balancing of single-loop mechanisms and parallel mechanisms that can be decomposed into two or more spherical kinematic chain units through mass moment substitution of a link [40-43] in Section 4.

3.2 Example 1: static balancing of single-loop spherical mechanisms

For the purpose of static balancing, a single-loop spherical mechanism can be turned into one or two spherical kinematic chain units by disconnecting an R joint. Using the results from Section 3, one can readily obtain that each link of a spherical kinematic chain unit can be statically balanced using one spring. Taking the spherical 5R mechanism as an example, we can remove anyone R joint of the mechanism for static balancing. When removing R_5 [in Fig. 7(a)], the mechanism turns into a serial spherical 4R manipulator, and each moving link of the mechanism is balanced using one spring. The spring connecting points on the base for balancing link 1 can be any point right above the joint axis of R_1, as shown in Fig. 7 [Eqs. (16-18)]. One can also divide the spherical 5R linkage into two spherical chain units composed of R_1 and R_2, and R_5 and R_4 respectively by removing R_3. The conditions for the static balancing of these two spherical kinematic chain units can be obtained using the results in Section 3.1.
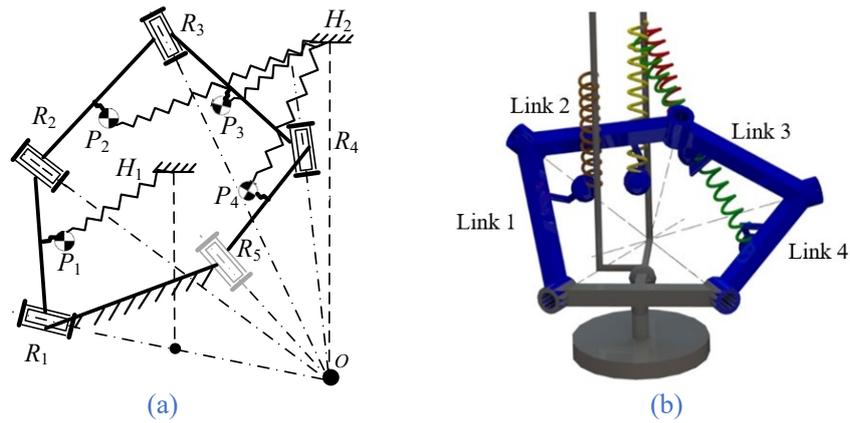
(a)　　　　　　　　　　　　　　(b)

Fig. 7 Statically balanced spherical 5R mechanism: (a) the sketch of the mechanism; (b) the 3D model of the mechanism

3.3 Example 2: static balancing of double-spherical mechanism
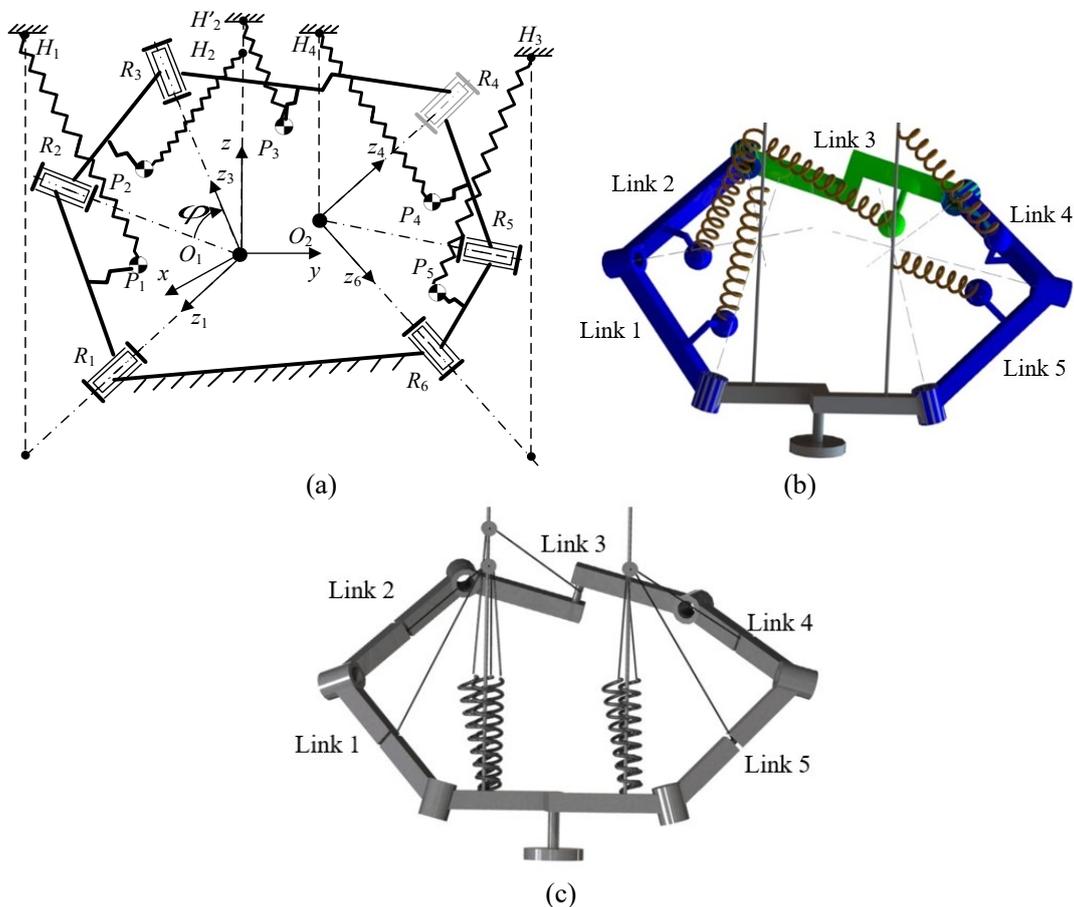

(a)　　　　　　　　　　　　　　(b)

(c)

Fig. 8 Statically balanced Bennett 6R double-spherical mechanism: (a) the sketch of the mechanism; (b) the 3D model of the mechanism (the special case when the spring attachment points on the base for balancing links 1 and 5 are right above O_1 and O_2 respectively); (c) the practical design of the system

The above static balancing approach is not limited to single-loop spherical mechanisms. This section will deal with the static balancing of a 1-DOF Bennett 6R double-spherical mechanism [37-39] (Fig. 8). In this mechanism, the joint axes of R_1, R_2 and R_3 intersect at O_1, and the joint axes of R_4, R_5 and R_6 intersect at O_2 (also double-RCM mechanism). Unlike a single-loop spherical linkage, one can only remove a specific R joint to turn the Bennett 6R double-spherical

mechanism into two spherical kinematic chain units. The mechanism can be divided into two spherical kinematic chain units composed of R_1, R_2 and R_3, and R_6 and R_5 respectively by removing R_4 (or two spherical chain units composed of R_1 and R_2, and R_6, R_5 and R_4 respectively by removing R_3). H_1 is a point right above the axis of R_1, and H_2 and H'_2 are two points right above O_1. The masses of the links in the first spherical kinematic chain unit are balanced by connecting H_1 and the CM of link 1, H_2 and the CM of link 2, and H'_2 and the CM of link 3 using three springs respectively. Similarly, the second spherical kinematic chain unit can also be balanced as shown in Fig. 8. Suppose the masses of links 1, 2, 4 and 5 are m and that of link 3 is m', and the CM of each link is at the centre of the link, a prototype is designed, as shown in Fig. 8(c). Rollers and cables are used to achieve zero-free-length springs [34]. The heights of H_1, H_2, H_3 and H_4 are mg/k and that of H'_2 is $m'g/k$.

If the two spherical kinematic chain units of the Bennett 6R double-spherical mechanism have the same parameters as the 2-DOF/3-DOF spherical manipulators in Section 2, fewer springs will be required for the static balancing.

4　Static balancing method of the mechanisms constructed using spherical chain units and other types of chain units

Not all the mechanisms can be turned into spherical kinematic chain units by removing R joints only. This section will focus on the static balancing of mechanisms that can be decomposed into spherical kinematic chain units and other types of chain units through mass moment substitution of a link [40-43]. First, the mass moment substitution approach [40-43] will be recalled in order to turn the static balancing of several mechanisms into those of several serial or tree-like kinematic chains. Then, the conditions for the static balancing of these mechanisms can be readily obtained using the results from Sections 2 and 3. Two examples will be given to illustrate the method.

4.1 Mass moment substitution approach

The mass moment substitution results for the RR links with two parallel joint axes, intersecting axes or skew axes [40-43] will be presented below.

4.1.1 Mass moment substitution of an RR link with parallel joint axes

The mass moment substitution of an RR link with parallel joint axes is shown in Fig. 9. The joint axes of R_i and R_{i+1} are parallel. The ith local coordinate frame is set at O, which is a point on the axis of R_i. z_i is along the joint axis of R_i and x_i is perpendicular to the plane defined by R_i and R_{i+1}. Suppose that the distance between R_i and R_{i+1} is t_0, the position vectors of the two point-masses expressed in the ith local frame are [40]

$$\begin{cases} {}^i\boldsymbol{P_{i1}} = \{0 \quad 0 \quad t_1\}^T \\ {}^i\boldsymbol{P_{i2}} = \{0 \quad t_0 \quad t_2\}^T \end{cases} \tag{19}$$
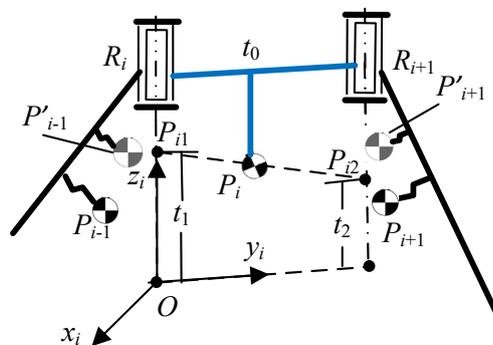

Fig. 9 Mass moment substitution of the RR link with parallel joint axes

The mass and mass moment (about O) of link i should be equal to those of the two point-masses. Therefore

$$\begin{cases} m_i = m_{i1} + m_{i2} \\ m_i g\ {}^iP_i = m_{i1}g\ {}^iP_{i1} + m_{i2}g\ {}^iP_{i2} \end{cases} \tag{20}$$

The following conditions can be obtained by solving Eq. (20).

$$\begin{cases} a_i = 0 \\ t_1 = (c_i t_0 - b_i t_2)/(t_0 - b_i) \\ m_{i2} = m_i b_i / t_0 \\ m_{i1} = (m_i c_i - m_{i2} t_2)/t_1 \end{cases} \tag{21}$$

where $\{a_i \quad b_i \quad c_i\}^T$ represents the position of CM of the ith link with respect to the ith local coordinate frame.

The mass of the RR link with parallel joint axes can be replaced by two equivalent masses on the two R joints when the CM of the link is on the plane defined by the two axes of the R joints ($a_i = 0$). Besides, the CM of the link and the two equivalent masses should be collinear ($t_1 = (c_i t_0 - b_i t_2)/(t_0 - b_i)$). The position of CM of the augmented $(i$-1$)^{th}$ link in the $(i$-1$)^{th}$ local frame can be obtained by combining the mass moment of the $(i$-1$)^{th}$ link and the first mass-point.

$$^{i-1}P'_{i-1} = (m_{i-1}g^{i-1}P_{i-1} + m_{i1}g^{i-1}P_{i1})/(m_{i-1} + m_{i1})g \tag{22}$$

Similarly, the CM of the augmented $(i$+1$)^{th}$ link in the $(i$+1$)^{th}$ local frame can be calculated by

$$^{i+1}P'_{i+1} = (m_{i+1}g^{i+1}P_{i+1} + m_{i2}g^{i+1}P_{i2})/(m_{i+1} + m_{i2})g \tag{23}$$

The positions of the CMs of the augmented links in the local frames are then obtained.

4.1.2 Mass moment substitution of an RR link with intersecting joint axes

An RR link with intersecting joint axes is shown in Fig. 10. The joint axes of R_i and R_{i+1} intersect at O. The angles between R_i and R_{i+1} are noted as α, the position vectors of the two mass-points in the ith local frame can be yielded as [41]

$$\begin{cases} {}^iP_{i1} = \{0 \quad 0 \quad t_1\}^T \\ {}^iP_{i2} = \{0 \quad t_2 S\alpha \quad t_2 C\alpha\}^T \end{cases} \tag{24}$$
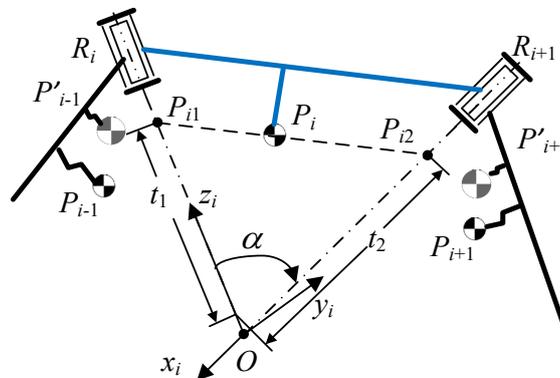
Fig. 10 Mass moment substitution of the RR link with two intersecting joint axes

The following conditions are obtained by substituting Eq. (24) into Eq. (20).

$$\begin{cases} a_i = 0 \\ t_1 = t_2 C\alpha (c_i tan\alpha - b_i)/(t_2 S\alpha - b_i) \\ m_{i2} = m_i b_i / t_2 S\alpha \\ m_{i1} = (m_i c_i - m_{i2} t_2 C\alpha)/t_1 \end{cases} \tag{25}$$

It is observed that the mass moment substitution conditions are: the CM of the link and the two R joints are coplanar, and the CM of the link is on the line defined by the two mass-points.

4.1.3 Mass moment substitution of an RR link with skew joint axes

An RR link with skew joint axes is shown in Fig. 11. The angle and distance between R_i and R_{i+1} are denoted as α and t_0 respectively. O_{2P}, P_{i2P} and R_{ip} are the projections of O_2, P_{i2} and R_i on the $z_i y_i$ plane.
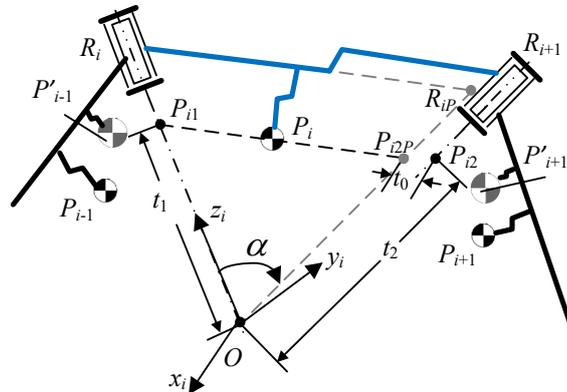

Fig. 11 Mass moment substitution of the RR link with skew joint axes

The position vectors of the two mass-points relative to the ith local coordinate frame are represented by [42, 43]

$$\begin{cases} {}^{i}\boldsymbol{P_{i1}} = \{0 \quad 0 \quad t_1\}^T \\ {}^{i}\boldsymbol{P_{i2}} = \{t_0 \quad t_2 S\alpha \quad t_2 C\alpha\}^T \end{cases} \tag{26}$$

The masses and the positions of the two point-masses are obtained as

$$\begin{cases} m_{i2} = m_i a_i / t_0 \\ m_{i1} = (m_i c_i - m_{i2} t_2 C\alpha)/t_1 \\ t_2 = b_i t_0 / a_i S\alpha \\ t_1 = t_0 (c_i \tan\alpha - b_i)/\tan\alpha (t_0 - a_i) \end{cases} \tag{27}$$

The CM of the link and the two masses point should be collinear.

4.2 Example 3: static balancing of Bennett plano-spherical hybrid linkage

Based on the mass moment substitution method, the 1-DOF single-loop reconfigurable Bennett plano-spherical hybrid linkage [38, 44] (Fig. 12) can be balanced. The axes of joints R_1, R_2 and R_3 are parallel, and those of R_4, R_5 and R_6 intersect at point O. Links 1, 3, 4 and 5 can be easily balanced based on the proposed methods. The mass of link 2 can be replaced by two point-masses on the joint axes of R_2 and R_3, then the mechanism is equivalent to two manipulators with payloads, including one 1-link manipulator mounted on R_1, and one spherical chain unit composed of R_4, R_5 and R_6.

H_1 is a point right above the axis of R_1, and H_2 and H'_2 are two points right above the intersection of the axes of R_4, R_5 and R_6. Four springs are used, one is attached to H_1 and to the CM of the augmented link 1 (combining the mass of link 1 and the first point-mass of link 2); the other three are attached to H_2 and the CMs of links 4 and 5, and H'_2 and the CM of the augmented link 3 respectively. It is noted that the spring attachment point on the base for balancing link 5 can be any points on the line right above R_6, as shown in Fig. 12(a). Suppose the masses of links 1, 2, 4 and 5 are m and that of link 3 is $m/2$, and the CM of each link is at the centre of the link. A prototype is designed, as shown in Fig. 12(c). When distributing the mass of link 2 to links 1 and 3, the spring attachment points on links 1 and 3 are at the top third of link 1 and top quarter of link 3 respectively. The masses of augmented links 1 and 3 are $3m/2$ and m respectively. The height of H_1 is $3mg/2k$ and those of H_2, H'_2 and H_3 are mg/k.
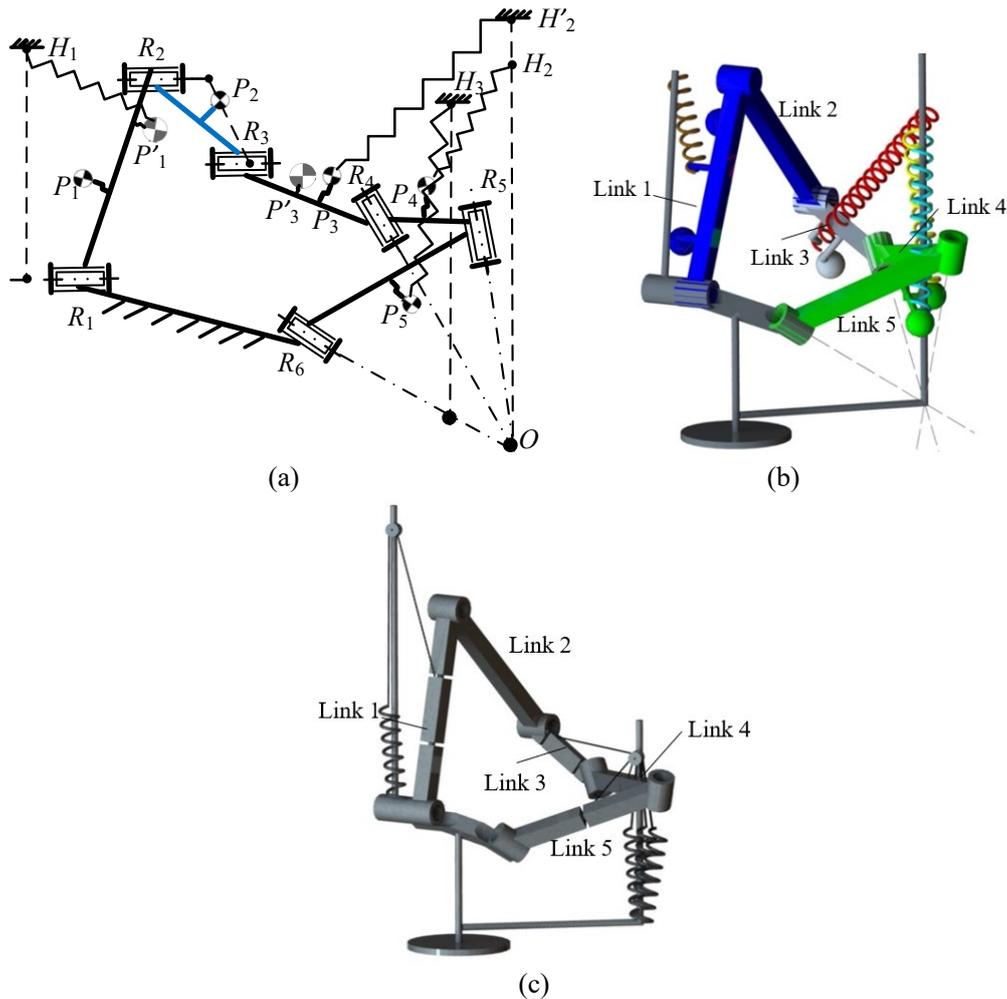
(a)

(b)

(c)

Fig. 12 Statically balanced Bennett plano-spherical hybrid linkage: (a) the sketch of the mechanism; (b) the 3D model of the mechanism (the special case when the spring attachment point for balancing link 5 is right above O); (c) the practical design of the system

4.3 Example 4: static balancing of 3-RRS parallel mechanism

A 3-DOF 3-RRS spherical PM, composed of two platforms and three RRS chains [45-46], is shown in Fig. 13. The axes of two R joints in each chain intersect at a point. Different from the spherical mechanism in [15], the axes of the R joints have no common point and the mechanism has no fixed centre of rotation. The two links in each chain are easily balanced by attaching the springs to the point right above the point of intersection and to the CMs of the links. To balance the upper platform, the mass of the upper platform is replaced by three point-masses located at the three S joints on the platform. The mass and mass moment (about O) of the upper platform should be equal to those of the three point-masses [Fig. 14(a)].

$$\begin{cases} m_u = m_{u1} + m_{u2} + m_{u3} \\ m_{u1}g(0, r_1C\varphi_1, r_1S\varphi_1) + m_{u2}g(0, r_2C\varphi_2, r_2S\varphi_2) + m_{u3}g(0,0,-r_3) = 0 \end{cases} \quad (28)$$

which leads to

$$\begin{cases} m_{u1}r_1C\varphi_1 + m_{u2}r_2C\varphi_2 = 0 \\ m_{u1}r_1S\varphi_1 + m_{u2}r_2S\varphi_2 - m_{u3}r_3 = 0 \end{cases} \quad (29)$$

Since the mechanism is symmetrically distributed,

$$\begin{cases} r_1 = r_2 = r_3 \\ \varphi_1 + \varphi_2 = \pi \end{cases} \quad (30)$$

Substituting Eq. (30) into Eq. (29), it is obtained that $m_{u1} = m_{u2} = m_{u3} = m_u/3$. By replacing the mass of the upper platform with the three point-masses, the parallel mechanism is equal to three 2R spherical chain units with payloads. The mass of the first spherical kinematic chain unit is balanced by connecting H_{11} (the point right above the axes of R_{11}) and P_{11}, the CM of

11

link 11, and H_{12} (the point right above the intersection of the axes of the two R joints) and P'_{12}, the CM of the augmented link 12 (combining the point masses of the upper platform and link 12) using two springs respectively (Fig. 14(b)). Similarly, the other two spherical kinematic chain units can also be balanced.
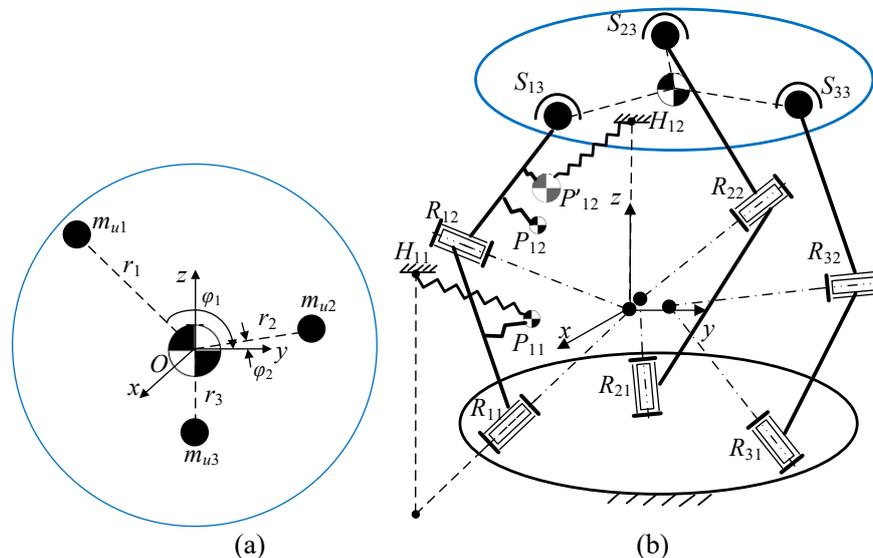

Fig. 14 Statically balanced 3-RRS parallel mechanism: (a) mass moment substitution of the upper platform; (b) the sketch of the mechanism

5 Discussion

The mechanisms in this paper can be balanced using fewer springs through the mass moment substitution. However, it is out of the scope of this paper for optimal static balancing of these mechanisms. In the future, the optimal static balancing of spatial manipulators using springs and counterweights will be investigated, and prototypes will be fabricated for applications of minimally invasive surgery. Since the mechanisms are constructed using spherical chain units, the mechanisms have remote center-of-motion (RCM) kinematics, which means the link always rotates around a fixed point. This characteristic can guarantee the safety of minimally invasive surgery. During the surgery, which often takes several hours, the static balancing can save the labor to hold and bring more stable operation. The double-spherical mechanism, which has two RCM center, can be applied to eye surgery. One is to track the eye movement while the other holds the surgical tool [47].

6 Conclusion

This paper has presented a geometric method for static balancing of spherical manipulators and mechanisms constructed using spherical kinematic chain units. The spherical chain units are composed of n moving links connected by R joints whose axes intersect at a point. Each moving link of the manipulator is balanced by connecting the point right above the point of intersection and the equivalent CM of the link using one spring. It is noted that the connecting point on the base for the first link can be any point right above the first joint axis. Using the proposed method, all the mechanisms constructed using spherical chain units can be readily balanced using only springs, with almost no calculation. The spherical 5R linkage and the double-centered Bennett hybrid 6R mechanism have been balanced as examples to illustrate the proposed balancing method.

In the cases that the mechanism is constructed using spherical chain units and other chain units, the method still works by distributing the mass of a link onto its adjacent links. Two examples have been provided, including a Bennett plano-spherical hybrid linkage and a 3-RRS parallel mechanism. By replacing the mass of one link with two point-masses, the mechanisms can be readily balanced by first turning the mechanism into several spherical kinematic chain units.

The static balancing of mechanisms that cannot be decomposed into spherical kinematic chain units by removing R joints or mass moment substitution of links deserves further investigation.

Acknowledgment

Appendix A Static balancing of 2-link manipulators

The total potential energy of the 2-link manipulators will be calculated in Appendix A. A fixed coordinate frame is attached to the base, with its origin at the intersection of the axes of the R joints, and z-axis is pointing vertically upward.
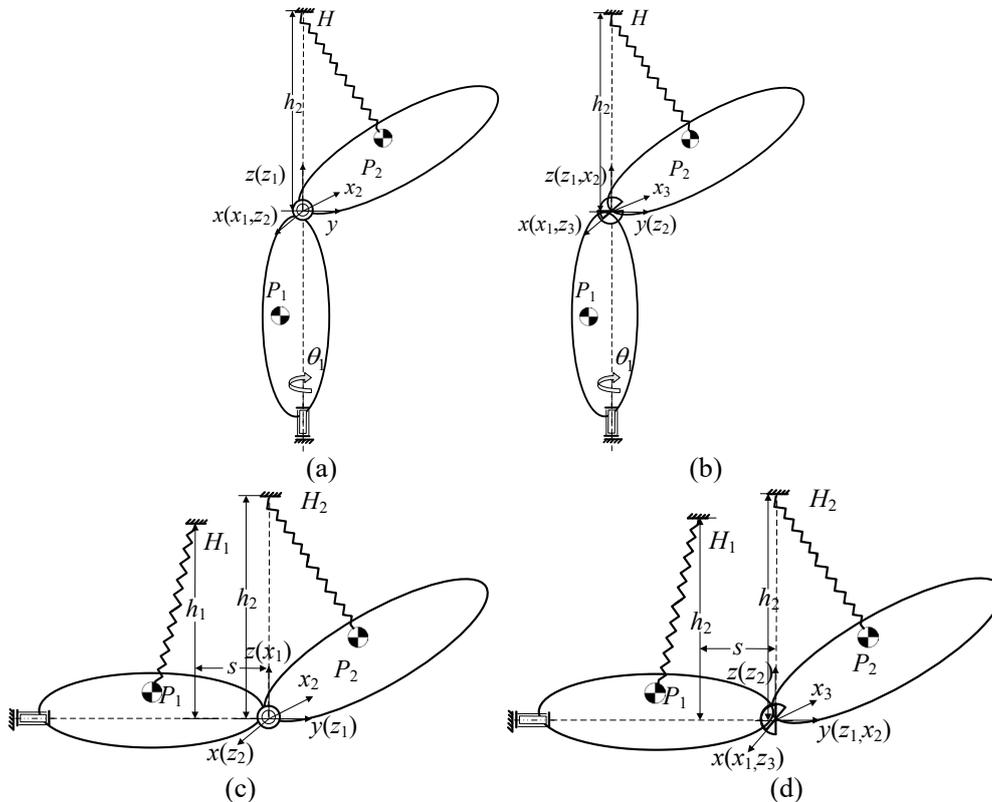

Fig. A1 Statically balanced 2-link manipulator: (a) yaw-roll rotation; (b) yaw-pitch-roll rotation; (c) pitch-roll rotation; (d) pitch-yaw-roll rotation

A1 Manipulators with yaw-roll rotation

The 2-DOF manipulator with yaw-roll rotation is shown in Fig. A1(a). Suppose that $\{a_i\ b_i\ c_i\}^T$ is the position of CM of the ith link in the local coordinate frame. The position vectors of the CMs of the two links in the global coordinate frame are calculated as

$$\begin{Bmatrix} P_1 \\ 1 \end{Bmatrix} = \{a_1 C\theta_1 - b_1 S\theta_1 \quad b_1 C\theta_1 + a_1 S\theta_1 \quad c_1 \quad 1\}^T \tag{A1}$$

$$\begin{Bmatrix} P_2 \\ 1 \end{Bmatrix} = \{P_{2x} \quad P_{2y} \quad -b_2 C\theta_2 - a_2 S\theta_2 \quad 1\}^T \tag{A2}$$

where

$$P_{2x} = a_2 C\theta_1 C\theta_2 - c_2 S\theta_1 - b_2 C\theta_1 S\theta_2$$
$$P_{2y} = -b_2 S\theta_1 S\theta_2 + c_2 C\theta_1 + a_2 C\theta_2 S\theta_1$$

Only one spring is needed to balance the manipulator. The spring connecting point H on the base is given by

$$\boldsymbol{H} = \{0 \quad 0 \quad m_2 g/k\}^T \tag{A3}$$

13

The total potential energy of the manipulator is obtained as

$$V = V_s + V_m = \frac{1}{2}k|\boldsymbol{P_2} - \boldsymbol{H}|^2 + m_2 g P_{2z} + m_1 g P_{1z}$$
$$= (a_2^2 k^2 + b_2^2 k^2 + c_2^2 k^2 + g^2 m_2^2)/2k + m_1 g c_1 \tag{A4}$$

which is constant. The system is thus statically balanced in any configurations.

A2 Manipulators with yaw-pitch-roll rotation

A 3-DOF manipulator with yaw-pitch-roll rotation is shown in Fig. A1(b). The position vectors of the CMs of the links in the global coordinate frame are

$$\begin{Bmatrix}\boldsymbol{P_1}\\1\end{Bmatrix} = \{a_1 C\theta_1 - b_1 S\theta_1 \quad b_1 C\theta_1 + a_1 S\theta_1 \quad c_1 \quad 1\}^T \tag{A5}$$

$$\begin{Bmatrix}\boldsymbol{P_2}\\1\end{Bmatrix} = \{P_{2x} \quad P_{2y} \quad b_2 C\theta_2 S\theta_3 - a_2 C\theta_2 C\theta_3 - c_2 S\theta_2 \quad 1\}^T \tag{A6}$$

where

$$P_{2x} = S\theta_1(b_2 C\theta_3 + a_2 S\theta_3) + C\theta_1[-c_2 C\theta_2 + S\theta_2(a_2 C\theta_3 - b_2 S\theta_3)]$$
$$P_{2y} = -C\theta_1(b_2 C\theta_3 + a_2 S\theta_3) + S\theta_1[-c_2 C\theta_2 + S\theta_2(-a_2 C\theta_3 + b_2 S\theta_3)]$$

The springs connecting point $\boldsymbol{H}$ on the base is

$$\boldsymbol{H} = \{0 \quad 0 \quad m_2 g/k\}^T \tag{A7}$$

The total potential energy of the system is a constant as

$$V = V_s + V_m = \frac{1}{2}k|\boldsymbol{P_2} - \boldsymbol{H}|^2 + m_2 g P_{2z} + m_1 g P_{1z}$$
$$= (a_2^2 k^2 + b_2^2 k^2 + c_2^2 k^2 + g^2 m_2^2)/2k + m_1 g c_1 \tag{A8}$$

A3 Manipulators with pitch-roll rotation

A manipulator with pitch-roll rotation is shown in Fig. A1(c). The position vectors of the CMs of the two links in the global coordinate frame are obtained as

$$\begin{Bmatrix}\boldsymbol{P_1}\\1\end{Bmatrix} = \{-b_1 S\theta_1 + a_1 C\theta_1 \quad c_1 \quad -a_1 S\theta_1 - b_1 C\theta_1 \quad 1\}^T \tag{A8}$$

$$\begin{Bmatrix}\boldsymbol{P_2}\\1\end{Bmatrix} = \{P_{2x} \quad -b_2 C\theta_2 - a_2 S\theta_2 \quad P_{2z} \quad 1\}^T \tag{A10}$$

where

$$P_{2x} = a_2 C\theta_2 C\theta_1 - b_2 C\theta_1 S\theta_2 - c_2 S\theta_1$$
$$P_{2z} = -a_2 S\theta_1 C\theta_2 - c_2 C\theta_1 + b_2 S\theta_1 S\theta_2$$

The springs connecting points $\boldsymbol{H_1}$ and $\boldsymbol{H_2}$ on the base are given by

$$\boldsymbol{H_1} = \{0 \quad -s \quad m_1 g/k\}^T \tag{A11}$$
$$\boldsymbol{H_2} = \{0 \quad 0 \quad m_2 g/k\}^T \tag{A12}$$

where s is the distance between $\boldsymbol{H_1}$ and z-axis. The total potential energy of the two links is

$$V_1 = V_{s1} + V_{m1} = \frac{1}{2}k|\boldsymbol{P_1} - \boldsymbol{H_1}|^2 + mg P_{1z}$$
$$= (a_1^2 k^2 + b_1^2 k^2 + c_1^2 k^2 + g^2 m_1^2 + 2c_1 s k^2 + s^2 k^2)/2k \tag{A13}$$

$$V_2 = V_{s2} + V_{m2} = \frac{1}{2}k|\boldsymbol{P_2} - \boldsymbol{H_2}|^2 + mg P_{2z} = (a_2^2 k^2 + b_2^2 k^2 + c_2^2 k^2 + g^2 m_2^2)/2k \tag{A14}$$

The results imply that the balancing method for the 2-link manipulators with pitch-roll rotation is valid.

A4 Manipulators with pitch-yaw-roll rotation

A manipulator with pitch-yaw-roll rotation is shown in Fig. A1(d). The position vectors of the CMs of the two links in the global coordinate frame are

$$\begin{Bmatrix}\boldsymbol{P_1}\\1\end{Bmatrix} = \{a_1 C\theta_1 - b_1 S\theta_1 \quad c_1 \quad -a_1 S\theta_1 - b_1 C\theta_1 \quad 1\}^T \tag{A15}$$

$$\begin{Bmatrix}\boldsymbol{P_2}\\1\end{Bmatrix} = \{P_{2x} \quad b_2 C\theta_2 S\theta_3 - a_2 C\theta_2 C\theta_3 - c_2 S\theta_2 \quad P_{2z} \quad 1\}^T \tag{A16}$$

where

$$P_{2x} = S\theta_1(b_2 C\theta_3 + a_2 S\theta_3) + C\theta_1[-c_2 C\theta_2 + S\theta_2(a_2 C\theta_3 - b_2 S\theta_3)]$$
$$P_{2z} = C\theta_1(b_2 C\theta_3 + a_2 S\theta_3) + S\theta_1[c_2 C\theta_2 + S\theta_2(-a_2 C\theta_3 + b_2 S\theta_3)]$$

The spring connecting points $\boldsymbol{H_1}$ and $\boldsymbol{H_2}$ on the base are

$$\boldsymbol{H_1} = \{0 \quad -s \quad m_1 g/k\}^T \tag{A17}$$
$$\boldsymbol{H_2} = \{0 \quad 0 \quad m_2 g/k\}^T \tag{A18}$$

The potential energy of the two links is

$$V_1 = V_{s1} + V_{m1} = \frac{1}{2}k|\boldsymbol{P_1} - \boldsymbol{H_1}|^2 + mgP_{1z}$$
$$= (a_1^2 k^2 + b_1^2 k^2 + c_1^2 k^2 + g^2 m_1^2 + 2c_1 s k^2 + s^2 k^2)/2k \tag{A19}$$

$$V_2 = V_{s2} + V_{m2} = \frac{1}{2}k|\boldsymbol{P_2} - \boldsymbol{H_2}|^2 + mgP_{2z} = (a_2^2 k^2 + b_2^2 k^2 + c_2^2 k^2 + g^2 m_2^2)/2k \tag{A20}$$

The results indicate that the manipulator with pitch-yaw-roll rotation is statically balanced through its range of motion.

Appendix B Static balancing of the 1-link manipulator

This appendix is to verify the spring connecting point on the link can be any point on the line defined by a point on the axis of the joint and the CM of the link, and that on the base can be any points right above the joint axis with a certain height. As shown in Fig. B1, $\boldsymbol{T}$ and $\boldsymbol{Q}$ are arbitrary points on the axis of the R joint, $\boldsymbol{H}$ is right above $\boldsymbol{Q}$, and $\boldsymbol{B}$ is a point on the line defined by $\boldsymbol{T}$ and $\boldsymbol{P}$. $OT = t$, $OQ = q$, $OP = r$, and $HQ = h$. The positions of $\boldsymbol{T}$, $\boldsymbol{H}$ and $\boldsymbol{P}$ are calculated as

$$\boldsymbol{T} = \{0 \quad 0 \quad t\}^T \tag{B1}$$
$$\boldsymbol{H} = \{0 \quad h \quad q\}^T \tag{B2}$$
$$\boldsymbol{P} = \{rC\theta \quad rS\theta \quad 0\}^T \tag{B3}$$
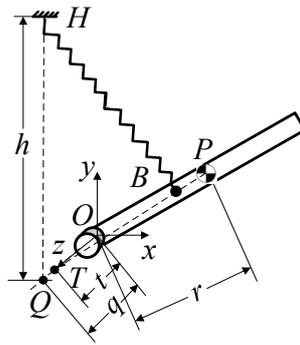
Fig. B1 Statically balanced 1-link manipulator

Suppose that $r(\boldsymbol{B} - \boldsymbol{T}) = b(\boldsymbol{P} - \boldsymbol{T})$ (the introduce of r is to simplify the equation, b/r is still an arbitrary value). We have

$$\boldsymbol{B} = \{bC\theta \quad bS\theta \quad (1 - b/r)t\}^T \tag{B4}$$

The total potential energy of the manipulator is yielded as

$$V = \frac{1}{2}k|\boldsymbol{B} - \boldsymbol{H}|^2 + mgP_y = \frac{1}{2}k[b^2 + h^2 + (t - bt/r - q)^2] - (kbh - mgr)S\theta \tag{B5}$$

The link is statically balanced when $h = mgr/kb$. The spring connecting point on the link can be any points on the line defined by $\boldsymbol{T}$ and $\boldsymbol{P}$, and that on the base can be any points right above the joint axis with a height of mgr/kb.

Appendix C Static balancing of spherical manipulators

The components of the position vector of P_3 in the spherical manipulator (Fig. 6) are

$$P_{3x} = -C\theta_1[C\theta_2(-a_3 C\theta_3 + b_3 S\theta_3) + S\theta_2(b_3 C\alpha_2 C\theta_3 + c_3 S\alpha_2 + a_3 C\alpha_2 S\theta_3)] - S\theta_1\{C\alpha_1[c_3 C\theta_2 S\alpha_2 + a_3 C\theta_3 S\theta_2 - b_3 S\theta_2 S\theta_3 + C\alpha_2 C\theta_2(b_3 C\theta_3 + a_3 S\theta_3)] + S\alpha_1[c_3 C\alpha_2 - S\alpha_2(b_3 C\theta_3 + a_3 S\theta_3)]\}$$

$$\tag{C1}$$

$$P_{3y} = -S\alpha_1[c_3 C\theta_2 S\alpha_2 + a_3 C\theta_3 S\theta_2 - b_3 S\theta_2 S\theta_3 + C\alpha_2 C\theta_2(b_3 C\theta_3 + a_3 S\theta_3)] + C\alpha_1[c_3 C\alpha_2 - S\alpha_2(b_3 C\theta_3 + a_3 S\theta_3)]$$

$$\tag{C2}$$

$$P_{3z} = c_3 S\alpha_2 S\theta_1 S\theta_2 + C\theta_1 S\alpha_1 S\alpha_2 (b_3 C\theta_3 + a_3 S\theta_3) + C\theta_2 S\theta_1 (-a_3 C\theta_3 + b_3 S\theta_3) - C\alpha_1 C\theta_1 [c_3 C\theta_2 S\alpha_2 + a_3 C\theta_3 S\theta_2 - b_3 S\theta_2 S\theta_3 + C\alpha_2 C\theta_2 (b_3 C\theta_3 + a_3 S\theta_3)] + C\alpha_2 [-c_3 C\theta_1 S\alpha_1 + S\theta_1 S\theta_2 (b_3 C\theta_3 + a_3 S\theta_3)]$$

$$(C3)$$

References

[1] R. H. Nathan, A constant force generation mechanism, ASME J. Mech., Transm., Autom. Des. 107(4) (1985) 508-512.

[2] A. T. Steinthorsson, M. E. Aguirre, G. Dunning, J. L. Herder, Review, categorization and comparison of 1 DOF static balancers, in: ASME 2015 International Design Engineering Technical Conferences and Computers and Information in Engineering Conference, Boston, 2015, pp. V05AT08A018-V05AT08A018.

[3] K. Koser, A cam mechanism for gravity-balancing, Mechanics Research Communications. 36(4) (2009) 523-530.

[4] B. G. Bijlsma, G. Radaelli, J. L. Herder, Design of a compact gravity equilibrator with an unlimited range of motion, Journal of Mechanisms and Robotics. 9(6) (2017) 061003.

[5] G. Carwardine, Equipoising mechanism, U.S. Patent No. 2,090,439. Washington, DC, 1937.

[6] M. J. French, M. B. Widden, The spring-and-lever balancing mechanism, George Carwardine and the Anglepoise lamp, Proceedings of the Institution of Mechanical Engineers, Part C: Journal of Mechanical Engineering Science. 214(3) (2000) 501-508.

[7] C. H. Kuo, S. J. Lai, Design of a novel statically balanced mechanism for laparoscope holders with decoupled positioning and orientating manipulation, Journal of Mechanisms and Robotics. 8(1) (2016) 015001.

[8] R. L. Smith, J. Lobo-Prat, H. van der Kooij, A. H. Stienen, Design of a perfect balance system for active upper-extremity exoskeletons, in: Rehabilitation Robotics (ICORR), 2013 IEEE International Conference, Seattle, 2013, pp. 1-6.

[9] A. Fattah, S. K. Agrawal, G. Catlin, J. Hamnett, Design of a passive gravity-balanced assistive device for sit-to-stand tasks, Journal of Mechanical Design. 128(5) (2006) 1122-1129.

[10] R. Rizk, S. Krut, E. Dombre, Design of a 3D gravity balanced orthosis for upper limb, in: Robotics and Automation, ICRA 2008. IEEE International Conference, Pasadena, 2008, pp. 2447-2452. IEEE.

[11] A. G. Dunning, J. L. Herder, A close-to-body 3-spring configuration for gravity balancing of the arm, in: Rehabilitation Robotics (ICORR), 2015 IEEE International Conference, Singapore, 2015, pp. 464-469.

[12] C. M. Gosselin, J. Wang, On the design of gravity-compensated six-degree-of-freedom parallel mechanisms, in: Robotics and Automation, 1998 IEEE International Conference, Leuven, 1998, pp. 2287-2294.

[13] J. Wang, C. M. Gosselin, Static balancing of spatial three-degree-of-freedom parallel mechanisms, Mechanism and Machine Theory. 34(3) (1999) 437-452.

[14] J. Wang, C. M. Gosselin, Static balancing of spatial four-degree-of-freedom parallel mechanisms, Mechanism and machine theory. 35(4) (2000) 563-592.

[15] C. M. Gosselin, Static balancing of spherical 3-DOF parallel mechanisms and manipulators, The International Journal of Robotics Research. 18(8) (1999) 819-829.

[16] J. L. Herder, Energy-free systems, Theory, conception and design of statically balanced mechanisms, Ph.D. thesis, Delft University of Technology, 2001.

[17] T. Van Dam, P. Lambert, J. L. Herder, Static balancing of translational parallel mechanisms, in: ASME 2011 International Design Engineering Technical Conferences and Computers and Information in Engineering Conference, Washington, 2011, pp. 883-889.

[18] P. Y. Lin, W. B. Shieh, D. Z. Chen, A stiffness matrix approach for the design of statically balanced planar articulated manipulators, Mechanism and Machine Theory. 45(12) (2010) 1877-1891.

[19] P. Y. Lin, Design of statically balanced spatial mechanisms with spring suspensions, Journal of Mechanisms and Robotics. 4(2) (2012) 021015.

[20] S. K. Agrawal, A. Fattah, Gravity-balancing of spatial robotic manipulators, Mechanism and machine theory. 39(12) (2004) 1331-1344.

[21] D. G. Chung, M. Hwang, J. Won, D. S. Kwon, Gravity compensation mechanism for roll-pitch rotation of a robotic arm, in: Intelligent Robots and Systems (IROS), 2016 IEEE/RSJ International Conference, Daejeon, 2016, pp. 338-343.

[22] G. J. Walsh, D. A. Streit, B. J. Gilmore, Spatial spring equilibrator theory, Mechanism and Machine Theory. 26(2) (1991) 155-170.

[23] C. Cho, W. Lee, J. Lee, S. Kang, A 2-dof gravity compensator with bevel gears, Journal of mechanical science and technology. 26(9) (2012) 2913-2919.

[24] S. H. Kim, C. H. Cho, Incomplete gravity compensator for a 4-DOF manipulator, Journal of Mechanical Science and Technology. 29(10) (2015) 4417-4426.

[25] Z. W. Yang, C. C. Lan, An adjustable gravity-balancing mechanism using planar extension and compression springs, Mechanism and Machine Theory. 92 (2015) 314-329.

[26] W. H. Chiang, D. Z. Chen, Design of planar variable-payload balanced articulated manipulators with actuated linear ground-adjacent adjustment, Mechanism and Machine Theory. 109 (2017) 296-312.

[27] S. Briot, V. Arakelian, A new energy-free gravity-compensation adaptive system for balancing of 4-DOF robot manipulators with variable payloads, in: Proceedings of the Fourteenth International Federation for the Promotion of Mechanism and Machine Science World Congress, Taipei, 2015.

[28] W. D. Van Dorsser, R. Barents, B. M. Wisse, J. L. Herder, Gravity-balanced arm support with energy-free adjustment, Journal of medical devices. 1(2) (2007) 151-158.

[29] W. D. Van Dorsser, R. Barents, B. M. Wisse, M. Schenk, J. L. Herder, Energy-free adjustment of gravity equilibrators by adjusting the spring stiffness, Proceedings of the Institution of Mechanical Engineers, Part C: Journal of Mechanical Engineering Science. 222(9) (2008) 1839-1846.

[30] B. M. Wisse, W. D. Van Dorsser, R. Barents, J. L. Herder, Energy-free adjustment of gravity equilibrators using the virtual spring concept, in: Rehabilitation Robotics, ICORR 2007. IEEE 10th International Conference, Noordwijk, 2007, pp. 742-750.

[31] R. Barents, M. Schenk, W. D. van Dorsser, B. M. Wisse, J. L. Herder, Spring-to-spring balancing as energy-free adjustment method in gravity equilibrators, Journal of Mechanical Design. 133(6) (2011) 061010.

[32] Y. L. Chu, C. H. Kuo, A single-degree-of-freedom self-regulated gravity balancer for adjustable payload, Journal of Mechanisms and Robotics. 9(2) (2017) 021006.

[33] P. Y. Lin, W. B. Shieh, D. Z. Chen, Design of a gravity-balanced general spatial serial-type manipulator, Journal of Mechanisms and Robotics. 2(3) (2010) 031003.

[34] D. A. Streit, B. J. Gilmore, 'Perfect' spring equilibrators for rotatable bodies, Journal of mechanisms, transmissions, and automation in design. 111(4) (1989) 451-458.

[35] J. Denavit, R.S. Hartenberg, A kinematic notation for lower-pair mechanisms based on matrices, Transactions of the ASME, Journal of Applied Mechanics. 22 (2) (1955) 215-221.

[36] G. J. M. Tuijthof, J. L. Herder, Design, actuation and control of an anthropomorphic robot arm, Mechanism and Machine Theory. 35(7) (2000) 945-962.

[37] L. Cui, J. S. Dai, Axis constraint analysis and its resultant 6R double-centered overconstrained mechanisms, Journal of Mechanisms and Robotics. 3(3) (2011) 031004.

[38] Y. Chen, Design of structural mechanisms, Ph.D. thesis, University of Oxford, 2003.

[39] G. T. Bennett, The parallel motion of Sarrus and some allied mechanisms, Philosophy Magazine. 6th series, 9 (1905) 803-810.

[40] T. Yang, Basic theory of mechanical system: structure, kinematic, and dynamic analysis, China Machine Press, 1996.

[41] X. Kong, Complete shaking force balancing of spherical mechanisms using mass moment substitution, Machine design (in Chinese). 14(8) (1997) 5-7.

[42] X. Kong, and T. -L. Yang, A mass moment substitution method for complete shaking force balancing of spatial linkages involving R and P pairs (I), Mechanical Science and Technology (in Chinese). 16(4) (1997) 575-580.

[43] X. Kong, and T.-L.Yang, Extensions to the mass moment substitution method for complete shaking force balancing of spatial linkages, in: Proceedings of 1998 ASME Design Engineering Technical Conferences, USA, 1998, DETC98/MECH-5846.

[44] K. Zhang, J. S. Dai, Screw-system-variation enabled reconfiguration of the Bennett plano-spherical hybrid linkage and its evolved parallel mechanism, Journal of Mechanical Design. 137(6) (2015) 062303.

[45] R. Di Gregorio, The 3-RRS wrist: a new, simple and non-overconstrained spherical parallel manipulator, Journal of Mechanical Design. 126(5) (2004) 850-855.

[46] X. Kong, C. M. Gosselin, Type synthesis of 3-DOF spherical parallel manipulators based on screw theory, Journal of Mechanical Design. 126(1) (2004) 101-108.

[47] G. Bai, P. Qi, K. Althoefer, D. Li, X. Kong, J. S. Dai, Kinematic analysis of a mechanism with dual remote centre of motion and its potential application. In: ASME 2015 International Design Engineering Technical Conferences and Computers and Information in Engineering Conference, 2015, pp. V05BT08A011-V05BT08A011.